Available online at www.sciencedirect.com
ScienceDirect
International Journal of Heat and Mass Transfer 50 (2007) 723–733
International Journal of HEAT and MASS TRANSFER
www.elsevier.com/locate/ijhmt

A dynamic study of steam-methane reforming

M.A. El-Bousiffi [a], D.J. Gunn [b,*]

[a] Libyan Petroleum Institute, National Oil Corporation, P.O. Box 6431, Tripoli, Libya
[b] Process Engineering Systems, P.O. Box 349, Swansea SA2 7YS, UK

Received 19 January 2006
Available online 20 September 2006

Abstract

Experiments have been performed on the catalysed steam reforming of methane in a computer-controlled micro-reactor over the temperature range 600–840 °C and the pressure range 2.5–9 atms. gauge. The principal operating method was dynamic in nature in which operating conditions were changed by computer program from the initial conditions to a second and sometimes a third or fourth set.

The reactor inputs were continuously measured by flow micro-controllers, and effluent flows were analysed by chromatography recorded at 15 min intervals over the period of an experiment. The total reaction period for more than 100 experiments was 600 h. Differential equations were set up to describe the axial composition profiles. Estimates of the kinetic constants were obtained from the entrance flows and exit reactor concentrations for each experiment.

A variability in the catalyst activity was found at temperatures less than 800 °C apparently due to activation of the catalyst at lower temperatures when there was an earlier period of operation at higher temperatures. Once the experiments affected by temperature activation had been excluded the experiments were found to be consistent in reproducing the effect of temperature, pressure, and composition.

Rate equations for the two dominant reactions were then obtained by functional analysis and non-linear parameter estimation from the flows and compositions for each consistent experiment.

Keywords: Methane; Reforming; Catalysis; Reactor; Spinel; Dynamic

1. Introduction

The steam reforming of natural gas is probably the most important process for the production of hydrogen and synthesis gas, base chemicals for many industrial processes. The first claim for nickel as a catalyst for the steam reforming of hydrocarbons was apparently made by Mond in 1889 [1], and the first industrial steam reformer was constructed by Standard Oil of New Jersey in 1931 [2]. The formulations of catalysts for the steam reforming of naptha fractions developed in the 1950s included high nickel content but catalysts subsequently developed for the commercial exploitation of natural gas were reduced in nickel content and operated at higher temperatures.

The modern commercial catalyst for primary reforming of natural gas is typically 10–25% nickel oxide with the remainder predominantly alumina. Catalyst pellets are usually cylindrical in shape of diameter 10–20 mm although the catalyst cylinder is often pierced by one or several holes parallel to the main axis. Commercial reaction conditions vary in the ranges of 600–900 °C and 5–40 bar. A high temperature culminating in a reactor exit temperature of 800–900 °C is necessary to overcome the adverse effect of lower temperatures on equilibrium yields. The effect of pressure is less significant. Equilibrium yields are improved at lower pressures, but operating pressures are often determined by the process requirements of downstream plant.

More recent kinetic studies using thermodynamically-consistent rate expressions, have been restricted to temperatures less than 600 °C while in earlier studies, although carried out at temperatures up to 900 °C, the kinetics have

* Corresponding author.
E-mail address: djgunn@ntlworld.com (D.J. Gunn).

0017-9310/$ - see front matter © 2006 Elsevier Ltd. All rights reserved.
doi:10.1016/j.ijheatmasstransfer.2006.07.006

Nomenclature

A	fractional conversion of methane	K_1	equilibrium constant for reaction 1, atm^2
B	fractional conversion of methane to carbon dioxide	K_2	equilibrium constant for reaction 2, atm^3
C_i	molar volume of component i, kmol/m^3	L	reactor length, m
c_1	number of moles of carbon monoxide in feed per mole of methane	N_0	total number of moles at reactor entrance per mole of methane feed
c_2	number of moles of carbon dioxide in feed per mole of methane	N_T	total number of moles per mole of methane feed
E_i	energy of activation for reaction i, kJ/kg mole	P	total absolute pressure, atms.
H	number of moles of hydrogen in feed per mole of methane	P_i	partial pressure of component i, atms.
k_1	reaction velocity constant for reaction 1, kmol/s m^3 atm^2	r_i	reaction rate kmol/s m^3
k_2	reaction velocity constant for reaction 2, kmol/s m^3 atm^3	R	universal gas constant, kJ/kg mole K
k_{10}	pre-exponential constant for reaction 1, kmol/s m^3 atm^2	s	number of moles of steam per mole of methane feed
k_{20}	pre-exponential constant for reaction 2, kmol/s m^3 atm^3	T	temperature, K
		U	velocity, m/s
		U_0	velocity at reactor entrance, m/s
		x	axial co-ordinate, m
		ϕ_i	defined by Eqs. (9) and (10)
		θ	$k_1 x/L$

often been expressed as pseudo-first order. It is a feature of the studies that there was a common difficulty in establishing a steady state for kinetic measurements. Catalyst activity declined sometimes sharply particularly at the outset, with measurements made at a time when the rate of decline was slower.

2. Resume of kinetic studies

Akers and Camp [3] studied the reaction between steam and natural gas within the temperature range of 340–640 °C at 1 atms. using 3 mm diameter pellets of nickel produced by the reduction of nickel oxide supported on kieselguhr. There was little reaction at temperatures less than 600 °C and they found first order dependence of the rate of disappearance of methane upon the partial pressure of methane at 640 °C.

Following studies of steam reforming of methane over nickel foil, Bodrov et al. [4,5], measured the kinetics of the reaction of methane with water vapour over a commercial catalyst – Giap-3, and a catalyst containing α-alumina impregnated with 4% nickel by weight. At 700 °C the kinetic data could be represented as first order with respect to methane, inhibited by adsorption of water and carbon monoxide in a similar manner to their findings on nickel foil. At temperatures within the range 700–900 °C a simple first order dependence was deemed sufficiently accurate. There was evidence of diffusional inhibition due to the size of the catalyst grains that ranged from 1.2–5.3 mm. The reaction was started at 700 °C after preliminary reduction with hydrogen and the activity gradually dropped for 30–40 h when a stationary value was reached. This stationary value was maintained at 700–800 °C for the remaining 40–100 h of the experiment.

Ross and Steel [6] studied reforming of methane over a co-precipitated nickel–alumina catalyst at temperatures between 500 and 680 °C in the pressure range from 1 to 10 Torr. Their results supported first order dependence of the rate of disappearance of methane upon methane partial pressure together with evidence of water inhibition.

Agnelli et al. [7] measured rates of reaction in a 10 mm diameter reactor between 642 and 738 °C. They reported similar findings to those of Bodrov et al. [5] including a decline in activity followed by attainment of a steady state after 40 h; they represented the kinetic data by similar expressions. In addition they observed that "after having worked at 738 °C, runs were performed at 642 °C, and it was noticed that the extent was remarkably higher than those previously determined, but declined to the previously obtained values, although slowly, with time on stream".

Xu and Froment [8] studied the steam reforming of methane over a crushed nickel–magnesium–alumina catalyst containing 15% nickel in a reactor of 10.7 mm diameter at temperatures between 500 and 575 °C and pressures between 5 and 15 bar. On the basis of their data they proposed three rate equations of thermodynamically-consistent form for the oxidation of methane by one mole of steam, by two moles of steam, and for the water gas shift reaction. The equations contained some 17 parameters determined by least squares estimation. After catalyst reduction in hydrogen at 810 °C for 12 h, the temperature was reduced to 575 °C. They reported that the catalyst activity dropped very quickly in the first 24 h, and then more gradually. The specific kinetic study was started after

70 h when deactivation was so slow that only minor adjustments were necessary to correct the kinetic data.

Soliman et al. [9] studied steam reforming of methane over a nickel–calcium aluminate-spinel catalyst in a commercial micro-reactor 6 mm in diameter at temperatures from 475 to 550 °C and pressures from 2 to 4 atms. The final rate equations proposed were similar in form to those of Xu and Froment [8] but the first equation for the oxidation of methane by 1 mol of steam was given a zero rate.

It is a feature of the studies that there was a common difficulty in establishing a steady state for kinetic measurements. Catalyst activity declined sometimes sharply particularly at the outset, with measurements made at a time when the rate of decline was slower. However the rate of decline was often great enough to require that kinetic measurements were corrected for the decline in activity over the period of the experiment. The decline in catalyst activity was usually attributed to "sintering" of the catalyst.

A common difficulty in the design and operation of the experimental tubular reactors was an upper limit of temperature that was significantly below the range of industrial interest. This is particularly true for the limits of 550 °C for Soliman et al. [9], and of 575 °C for Xu and Froment [8] that were also in a range found to show little reaction by Akers and Camp [3]. The temperature restrictions were not apparently due to temperature limitations of their equipment, but rather to upper gas velocity limits and lower limits on reactor size operating together so that equilibrium was attained in the reactor at temperatures above 550–575 °C and therefore kinetic measurements could not be made. The quartz recirculating reactor used by Bodrov et al. [4] was not restricted in this way and measurements could be made up to 900 °C.

In this paper we present some results from a dynamic study of a commercial nickel-based catalyst using a newly-developed micro-reactor operating under computer control. The physical size of the reactor was very small and as the flow capacity of the reactor system was high, equilibrium limitations were not as great. The range of operating temperature for which kinetic data were collected was 600–850 °C, and the range of operating pressure was 2.5–9 atms., both ranges well within the limits of the micro-reactor.

An important feature of the design of the reactor was the capability of introducing temperature and flow changes under computer control. This feature allowed the observation of temperature and composition dynamics over a range of time scales.

3. Experimental equipment and methods

The commercial catalyst used in this study was formed using calcium aluminate as a pellet-forming cement with a nickel salt used to impregnate the pellets before calcining to give nickel oxide. The hollow cylindrical pellets 10 mm in diameter containing 15% nickel oxide, 15% calcium oxide and 70% alumina by weight were crushed to form rough isometric particles 0.2–0.3 mm in size. The small catalyst size eliminated the effect of intraparticle diffusion. An experiment on the reactor without catalyst showed no detectable reaction.

A diagram of the experimental arrangement is shown as Fig. 1. The reactor consisted of a length of Inconel tube of 3 mm bore packed with catalyst. A mass of crushed catalyst was supported between ceramic wool plugs. The length of reactor was set by the mass of catalyst consolidated between the plugs and was measured to be 48 mm; the mass of catalyst was 0.45 g. Reactants were delivered to the reactor from standard pressurised gas cylinders each provided with a multistage pressure regulator, with individual flow controllers for each gas set by output signals from the

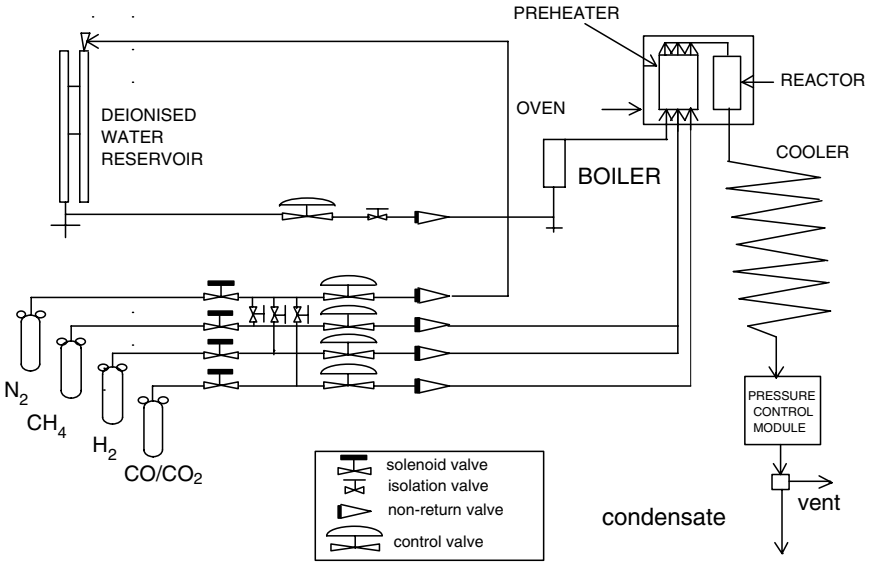

Fig. 1. Diagram of micro-reactor.

digital computer. The flow micro-controllers were each calibrated to an accuracy of ±1%.

Temperature control was arranged by passing the gases through a pre-heater, and delivering the gases at controlled temperature to the reactor. The reactor and pre-heater were each held in Inconel blocks surrounded by resistive heaters within insulated jackets. Thermocouples placed in each block registered the temperatures of the reactor and pre-heater, and the temperatures were fed into control loops with computer-generated control signals setting the power outputs to each resistive heater. Steam generation was arranged by feeding a controlled flow of nitrogen to a de-mineralised water reservoir displacing the same volumetric flow of demineralised water to a temperature-controlled boiler. Steam generated by the boiler was passed to the pre-heater, mixed with other reactants at the pre-heater outlet, and the combined stream was then fed to the reactor.

Outlet gases from the reactor passed into a high capacity cooler and thence into a pressure control module in which the pressure registered by a transducer was used to control the position of a variable-opening solenoid valve in the fluid effluent line. The signal from the transducer was used to maintain the system pressure at a pre-set value.

All the control settings and values of flow-rates, pressures and temperatures were displayed by the computer at chosen intervals. The programme for the reactor operation was arranged before the run by computer interrogation so that changes in temperature and flow settings could be made without operator intervention. This facility allowed process changes to be made under conditions of minimum disturbance.

The response times for temperature were obtained by changing the temperature set points. In a typical response the temperature initially set at 705 °C was changed to 795 °C and then to 701 °C. A new set point was achieved within 25 min to a precision of ±2 °C. The response time for the flow controllers was of the order of 10 ms. The response time for flow changes at the reactor taking into account the volumetric capacity of the system was of the order of 1 min, much less than the temperature response time.

From the outlet control valve, condensate was separated into a receiver for subsequent measurement, and the gases were passed to a bypass and sample valve that allowed sampling and elution of the dry sample into a chromatograph. A chromatograph column, 1.5 m long packed with Poropak Q, was installed into a temperature-controlled oven, an integral part of a Pye chromatograph fitted with a dual-port katharometer detector. The chromatograph was set up and calibrated for methane, carbon monoxide and carbon dioxide using hydrogen as the carrier gas, and calibrated for hydrogen using nitrogen as the carrier gas. In operation methane, carbon monoxide, carbon dioxide and hydrogen were determined from the chromatograms by means of the calibrations in the first stage of the investigation.

4. Aspects of the operating dynamics

The purpose of catalyst activation is to reduce nickel oxide to the catalytically active form, but a survey of industrial activation practice [1] showed a variety of methods, so that it was decided to activate at 700 °C for 18 h at a steam to hydrogen molar ratio of 7, and pressure of 5 bar gauge. Subsequent steam-methane reforming experiments were carried out for a total of 590 h using the same catalyst bed, but the choice of activation conditions was changed during the programme as will be described. The operating time was determined as the period during which methane was fed to the reactor and excluded preparation when the reactor was brought to operating conditions, and shutdown when the methane feed had been stopped and the reactor was cooled in a flow of hydrogen.

Equilibrium in the reforming process may be attained by the set of reactions,

$$CH_4 + H_2O \iff CO + 3H_2 \quad (1)$$

$$CH_4 + 2H_2O \iff CO_2 + 4H_2 \quad (2)$$

$$CO_2 + H_2 \iff CO + H_2O \quad (3)$$

The feed arrangements allowed the controlled flow of methane, steam, hydrogen, carbon monoxide and carbon dioxide to the reactor. From gas analyses, the stoichiometry, and equilibrium conditions for the set of reactions and the feed composition, the approach to equilibrium conversion of methane was calculated as the ratio of methane converted to that converted at equilibrium.

The approach to equilibrium was calculated by following the changes in composition from initial values according to the stoichiometry of reactions (1) and (2). By expressing the changes in composition at equilibrium from the initial composition and equating to the equilibrium constants, non-linear equations were obtained that were then solved by the method of linear interpolation to give compositions at equilibrium.

The reactor exit compositions obtained from chromatography were corrected for carbon and hydrogen material balances as given by the measured input flows of methane, steam, carbon monoxide and carbon dioxide to give corrected reactor exit flows and the fraction of methane converted.

The first three experiments were carried out at 700 °C at a methane flow-rate of 202 N ml/min, a steam to methane molar ratio of 2.94 and hydrogen to methane molar ratio of 0.5 at a pressure of 5 bar. The experiments produced exit gas compositions that could not be distinguished from equilibrium. However subsequent experiments within a few hours at the same conditions showed that equilibrium had not been attained evidently because there had been a fairly sharp decline from the initial level of catalyst activity.

The decline in catalyst activity continued in the early stages of reactor operation. Additional periods of activation were intermingled with the reforming experiments using a pattern of activation by a mixture of steam and

hydrogen as described in accounts of industrial practice. The hydrogen to methane feed ratio was set at 0.5 for the first 60 h of operation that included eleven separate runs of about 7 h duration from start-up to shutdown, each including about 6 h of reaction. After 40 h when the activity of the catalyst continued to decline the catalyst was reconditioned for periods from 1 to 15 h using steam and hydrogen, and hydrogen alone during the period from 40 to 60 h.

The conversion of methane for experiments in the first period of operation is shown in Fig. 2 when the initial reactor conditions were maintained at 700 °C, a methane flow-rate of 202 N ml/min, a steam to methane molar ratio of 3, and hydrogen to methane molar ratio of 0.5 at a pressure of 5 bar gauge. After three periods of activation by a mixture of steam and hydrogen, activation was carried out for two further periods by hydrogen alone as shown in the record. Although there was an initial increase of activity at 40 h, it is clear that the periods of conditioning did not apparently reduce the rate at which the activity declined and until 60 h the activity continued to decline in spite of catalyst reconditioning.

As there was no apparent benefit from the periods of activation, it was discontinued and after 60 h of operation the feed ratio of hydrogen to methane was increased to 1 from 0.5 with other reactor conditions unchanged. The dependence of the approach to equilibrium upon time for the first 135 h of reactor operation is shown in Fig. 2, and it is apparent that the catalyst activity had stabilised at a ratio of hydrogen to methane of 1 in the feed once the ratio had been increased from the operating time of 60 h.

It was now clear that although the period and procedures for shutdown were standard, the condition of the catalyst at start-up for subsequent runs varied, being affected possibly by the variable period of shutdown between runs. Reactor exit compositions could vary as much as 10% during the experiment. It was subsequently found that the variation in the steady-state composition could be reduced and a clearer pattern of experimental behaviour could be observed by introducing dynamic experimentation. After start-up in a dynamic experiment when a first steady state had been reached, changes in temperature, flow-rate or feed composition were introduced by computer program until a second steady state was reached. The experiment was then stopped or continued either by reverting to the first set of conditions, or introducing further changes in operating conditions.

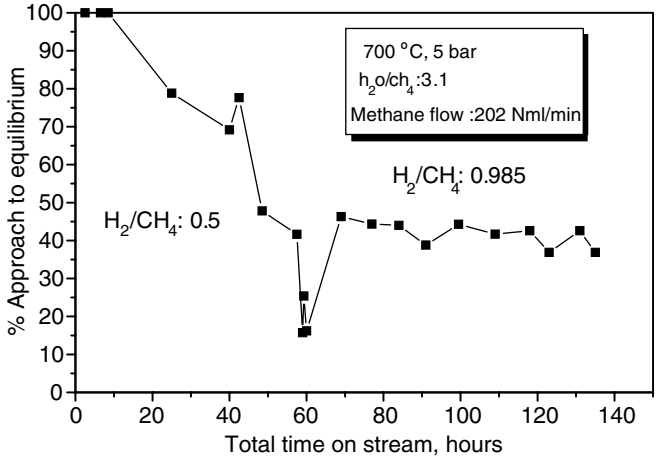

Fig. 2. Initial change in catalytic activity.

For the dynamic experiments it was necessary to simplify the analytical method because the time required for the full chromatographic analysis with two carrier gases allowed only a small number of gas analyses within the time-scale of a full experimental run from reactor start-up to shutdown. In the revised method the gas analysis was carried out using hydrogen as the carrier gas to measure methane, carbon monoxide, and carbon dioxide. The reactor exit flows of methane, carbon monoxide, and carbon dioxide were then determined from the chromatograms and a carbon balance using the accurately measured input of methane. The flow of hydrogen was found from the known accurate input of hydrogen to which was added the hydrogen produced in reaction (1) associated with the production of carbon monoxide, and the hydrogen produced in reaction (2) associated with the production of carbon dioxide. The flow of steam was found from the known accurate input of steam from which was deducted steam required for the production of carbon monoxide according to reaction (1), and steam required for the production of carbon dioxide according to reaction (2). With the exit flows established for each component, the exit gas composition was then calculated. Because of the accuracy of the micro-controllers in measuring the input flows of methane, hydrogen, and the balanced flow of nitrogen giving a steam flow of equivalent accuracy, an error analysis indicated that the limiting factor in the accuracy of the estimate of reactor gas compositions was the chromatographic measurement. Thus the use of a single carrier gas gave an improved accuracy and allowed the number of gas measurements to be doubled within the same time interval from the number that could be attained when two carrier gases were used.

Fig. 3 shows the composition response to a change in temperature from the initial setting of 840 to 797 °C followed by a return to 840 °C. Other operating conditions of feed composition, flow-rate and pressure were kept constant. The fall in temperature caused a reduction in the rate of methane oxidation, associated with a significant fall in carbon monoxide content. However the change in carbon dioxide concentration was slight. The time allowed for the development of each steady state was significantly greater than the time required to reach a new steady state in temperature. It is immediately evident that the effect of changes in operating conditions can readily be seen in this type of experiment provided that sufficient time is allowed for the different steady states to develop. This experimental procedure was adopted for subsequent experiments. In this

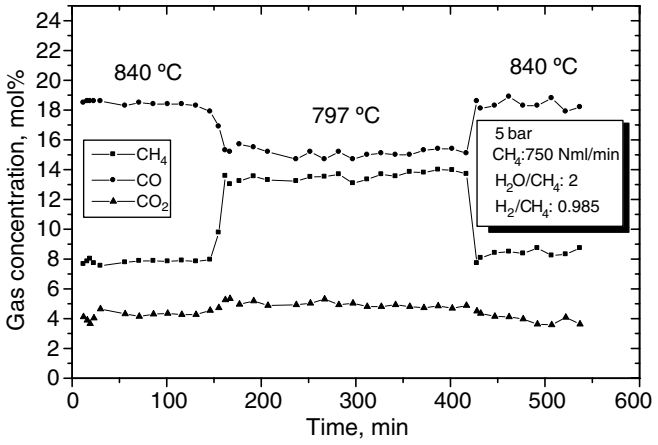

Fig. 3. Example composition dynamics.

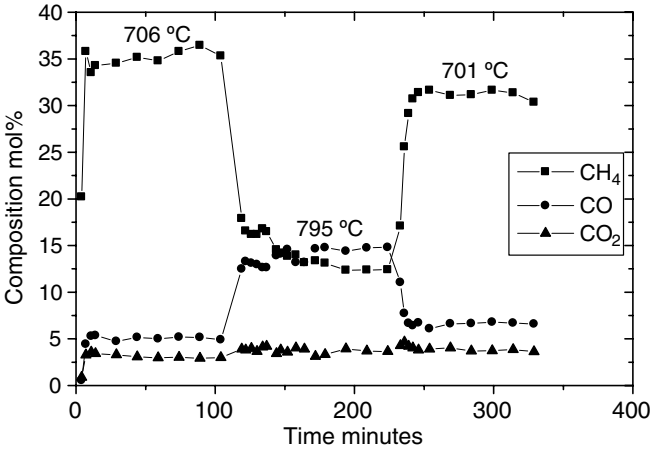

Fig. 5. Change of gas composition 706–795–701 °C.

particular example it appears that the step change from 840 to 797 °C and back to 840 °C was reversible and it is clear that steady state compositions have been obtained within the time scale dictated by the temperature dynamics.

Fig. 4 shows composition changes following a temperature change from 797 to 705 °C followed by a return to 797 °C. As with the changes illustrated in Fig. 3, steady levels of composition were reached in the time interval required for temperature stabilisation; the initial and final compositions at 797 °C are the same within the probable range of experimental error.

However a significant difference was observed when the changes in temperature levels were inverted. The effect of an inverse change for the same temperature levels is shown in Fig. 5 where it is clear that the composition changes were not reversible. The methane content in the reactor exhaust gas that was 35% at 706 °C had declined to 32% after the reactor temperature had been raised to 795 °C followed by a fall to 701 °C. The carbon monoxide showed a corresponding increase from 5% to 7% with the carbon dioxide unchanged by the temperature excursion at 3%. In subsequent operation at 700 °C the catalyst showed significantly enhanced activity for a time as great as 10–20 h. This was a clear effect of activation, and there was no evidence of the catalyst deterioration reported in the literature by researchers who worked at lower temperatures.

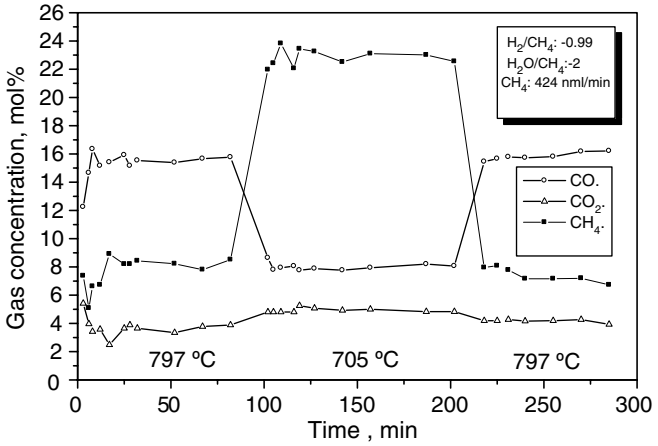

Fig. 4. Change of gas composition 797–705–797 °C.

The purpose of the dynamic experiments typically illustrated in Figs. 3 and 4 was to estimate steady-state kinetics from the later stages of each experiment following a change in computer-controlled conditions and this procedure was effective provided that no longer term change was present. However the variability in catalyst activity over long periods raised the acute difficulty of assessing the effect of operating variables upon intrinsic catalyst performance. To provide a benchmark against which the effect of variables such as steam to methane ratio could be assessed, it was decided to carry out standard experiments throughout the experimental programme as a continuous indicator of catalyst activity. The effect of operating variables outside the standard set could then be ascertained by employing the technique of dynamic experimentation, estimating each apparent steady state, and referring the results to the nearest standard experiment.

The standard experimental conditions were chosen as operating pressure of 5 bar gauge, methane flow-rate of 202 N ml/min, steam to methane ratio of 3 and hydrogen to methane ratio of 1 in the feed. Because of the apparent influence of high temperature upon subsequent experiments at lower temperature, the standard experiment was carried out at several temperatures, 600, 700, 750, and 800 °C.

The experimental record of the standard experiments expressed as apparent steady state equilibrium conversion of methane is shown from 50 to 500 h in Fig. 6. Other experimental conditions that were examined during this period are not shown in this figure. The different temperatures that were examined including further experiments at 840 °C, were chosen to cover the range of industrial interest.

There is a clear increase of catalytic activity at 700 °C once experiments at 800 °C were included. The insertion

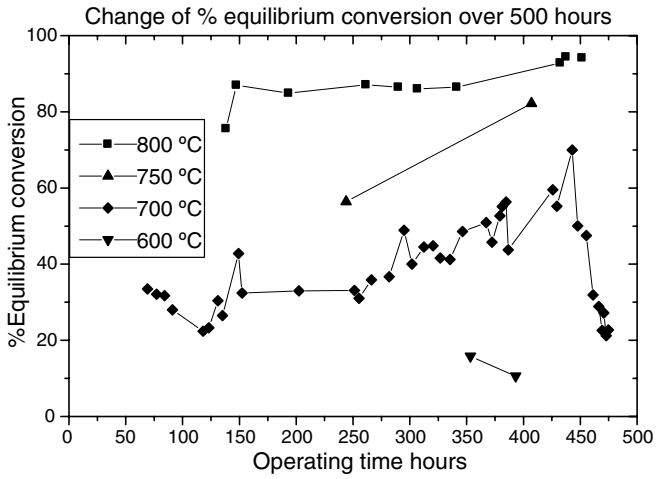

Fig. 6. Change of methane conversion over 500 h.

of four runs of about 30 h in duration at 800 °C spread over the period from 160 to 260 h increased conversion at 700 °C from 40% of equilibrium conversion of methane to approximately 55%. An increase in the frequency of runs at 800 °C over the period 260–340 h was associated with a further increase in conversion of methane at 700 °C to 70% of equilibrium. Operation at 800 °C was discontinued at 450 h and over the next 40–50 h conversion fell to 40% of equilibrium at 700 °C, the same conversion as was found over the period 70–130 h before any operation at 800 °C.

Evidently periods of reactor operation at 800 and 750 °C increased catalyst activity for subsequent operation at 700 °C with the level of enhancement dependent upon the frequency of operation at 750–800 °C. The increase in activity induced in this manner decayed with time falling to the unactivated condition some 20–40 h after activation. Increasing the frequency of operation at higher temperature reduced the rate of decline of activity at 700 °C leading to increased activity at the lower temperature as shown in Fig. 6. However the temperature activation was not sufficient to restore the activity found in the earliest operations and it appears that the initial decline as shown in Fig. 2 was irreversible.

The activity of the catalyst at 800 °C approached a steady value over the period 150–500 h in strong contrast to the variation of catalytic activity shown in operation at 700 °C.

In addition to measuring the effect of temperature upon reactor performance, the effects of pressure, reactor flowrate, steam to methane ratio in the feed, hydrogen to methane ratio in the feed, and carbon monoxide to methane ratio in the feed, were examined in a number of experiments. The concentration of the reacting gas varied from the inlet composition creating large variations in component ratios within the reactor so that the feed composition ratios extended the intrinsic scale of composition variations.

The catalyst particles were ≈0.2 mm in size, and ancillary calculations established that concentration gradients within the particles were slight, and the effect of axial mixing within the reactor [10] was small enough to be neglected when set against the levels of accuracy in the measurement of the reaction kinetics.

Further details of the experimental arrangement have been given by El-Bousiffi [11].

5. The variation of catalytic activity

It is a feature of laboratory investigations into nickel-catalysed steam reforming that changes in the catalytic activity of ceramic or cement supported nickel catalysts with time are commonly found [1]. Thus Agnelli et al. [7], Akers and Camp [3], Bodrov et al. [5], Ross and Steel [6], and Xu and Froment [8] have reported a decline in catalyst activity from the initial conditions. The decline is commonly attributed to catalyst sintering, although the experiments were often less than 100 h in duration and commercial catalysts can operate for periods of four years or so. In addition only Agnelli and Bodrov operated in the commercially important temperature range. Agnelli et al. also reported that operation at 738 °C enhanced activity at a lower temperature for a short period.

Takemura et al. [12] have examined the formation of nickel aluminium spinel from alumina and nickel oxide and the products of reduction by hydrogen and reforming gases using differential thermal analysis and X-ray analysis. The study followed dynamic changes in the phase compositions. The reduction followed the reaction:

$$NiO \cdot Al_2O_3 + H_2 \iff Ni + H_2O + Al_2O_3 \quad (4)$$

Tablets of dimension 6 mm consisting of 10% nickel oxide and α-alumina were fired at 1000 °C for 1 h and X-ray analysis showed that only alumina and spinel were present. Subsequent reduction by hydrogen at 700 °C showed that about 12% of the nickel was reduced to the metallic state but reduction at 970 °C showed only alumina and metallic nickel. If the catalyst was subsequently re-oxidised at 900 °C for 5 min and then reduced at 700 °C they found that the degree of reduction was increased to 38% from 12%, and at 800–850 °C the reduction of the spinel to metallic nickel was substantially complete. The increased catalyst reduction at 700 °C in the second case was attributed to crystal fragmentation of the catalyst occasioned by the previous reduction and subsequent oxidation.

In tests on catalytic activity they found that nickel in a catalyst showing a high activity occurred mainly in metallic form, and there was no apparent difference in activity between catalysts reduced by hydrogen and reduced by reforming gases.

In another study it has been found that electron micrographs of reduced catalyst showed nickel crystals of nearly ideal sixfold symmetry of size 15–150 nm [1].

The catalyst used in this investigation was formed as an alumina support with nickel added by impregnating the support with a nickel salt with calcium aluminate as a cement binder. In the first stage of reduction, microcrystalline nickel

would be precipitated throughout the support from the highly dispersed nickel oxide, giving a high surface area of nickel and hence a high catalytic activity. The high initial activity is shown in Fig. 2. The highly dispersed nickel then reacted with the catalyst support forming nickel aluminium spinel that according to the investigation of Takemura would be largely unreduced at 700 °C. The initial high activity due to microcrystalline nickel disappeared because of recrystallisation and the formation of spinel over the early experimental period. The decline in reactivity was halted but not reversed by increasing the hydrogen to methane ratio to 1 as shown in Fig. 2. Evidently the activity of the catalyst depends upon the hydrogen to steam ratio as well as temperature with a hydrogen to steam ratio of 0.33 at the reactor inlet showing a significant improvement in catalyst activity compared to an inlet ratio of 0.165.

The initial high catalytic activity is due to the formation of micro-crystallites of nickel throughout the catalyst structure arising from the micro-distribution of nickel throughout the catalyst in manufacture. The reactivity falls because of the effect of solid-state diffusion allowing the nickel to react with alumina to form spinel. The level of reduction of the spinel is only raised by an increase in the hydrogen content of the feed gases from 60 h as shown in Fig. 2.

Takemura's conclusion that a temperature of 800 °C or greater is necessary for the complete reduction of nickel spinel is in accord with changes in the activity of the catalyst found in this investigation. As shown in Fig. 5 an increase in temperature of the catalyst from 706 to 795 °C has accomplished a further reduction of the catalyst that persists when the temperature is reduced to 701 °C. Subsequently the catalyst slowly reoxidises over a period of several hours if the reaction is continued at the lower temperature.

Changes in the activity of the catalyst over a much longer period are illustrated in Fig. 6. Alternation in the operation of the reactor between 700 and 800 °C from 150 to 440 h caused a large increase in activity at 700 °C due to the enhanced catalyst reduction experienced at 800 °C. The figure also shows that catalyst activity at 800 °C is reduced to a small extent when experiments at 700 °C are intermingled with experiments at the higher temperature. Takemura's study suggests that catalyst reduction is substantially complete at 800–850 °C. Once the operation at 800 °C was discontinued the catalyst activity at 700 °C reverted to the level measured before the start of experiments at 800 °C.

The catalyst activity at 700 °C from 150 h shows a gentle increase at first because of the low frequency of 800 °C experiments. As the frequency of experiments at the higher temperature increases there is a corresponding increase in the catalyst activity until experiments at 800 °C were stopped when the activity at 700 °C fell to the value at 150 h. If the initial period and the effects of temperature enhancement at 700 °C between 250 and 475 h are excluded, the catalyst performance appears to be stable. At the end of the experiments the catalyst was still free-flowing and there was no trace of sintering or coking.

6. Estimation of reaction kinetics for industrial applications

The principal purpose of the experiments was to obtain kinetic information over a range of operating conditions for application in the design and operation of full-scale reactors, but it is apparent that laboratory measurements in batch experiments show influences that are not present in large scale reformers.

The temperature distribution along the length of an industrial primary reformer increases from 500–600 °C at the entrance to 800–900 °C at the reactor exit, and enhancement of kinetics in the industrial reactor at 700 °C by earlier operation at 800 °C does not normally occur; neither are the kinetics at 800–900 °C affected by preceding operation at 700 °C. Thus kinetic measurements made in the experimental reactor have to be selected to exclude the effect of temperature enhancement and the commonly found initial decline in activity, before possible application to the industrial reactor.

The standard kinetics at 800 °C were obtained as the condition established over the period 150–500 h, and the standard kinetics at 750 °C were established as the condition attained at 200 h. The measured kinetics at 700 °C chosen for the data set were obtained from standard experiments between 60 and 140 h of operation before any experiments at 750 and 800 °C had been carried out. Further experiments at 700 °C beyond 475 h that were not affected by earlier operation at higher temperatures were also included. In addition, a set of experiments at 840 °C was performed in the latter stages of the experimental programme. However because of the effect of temperature enhancement that would not be reproduced in the industrial-scale reactor, experiments at 700 °C for the period from 250 to 475 h as shown in Fig. 6, were excluded. The initial experiments in the first 50 h of operation were also excluded.

The data set for kinetic analysis contained the results of more than 70 experiments including not only some 30 allowable experiments shown in Fig. 6, but a set at different flow-rates over the range from 202 to 750 N ml/min, while independently changing the inlet molar ratio of steam to methane flow between 2 and 3.2, and the inlet molar ratio of hydrogen to methane flow between 0.5 and 2.

The kinetic analysis was based upon a numerical study of chemical reactions (1) and (2) that were promoted during axial flow through the bed of catalyst; all three reactions were considered but it was found that an analysis that specifically included reaction (3) gave no improvement in describing the kinetics. The reactor may be considered to be isobaric and isothermal under the conditions of operation, and the effects of intra-particle diffusion and axial dispersion may be neglected.

The two differential equations that describe the progress of reactions along the tubular reactor are,

$$r_1 = \frac{\mathrm{d}}{\mathrm{d}x}(UC_{\mathrm{CH_4}})_1 = -k_1\left(P_{\mathrm{CH_4}}P_{\mathrm{H_2O}} - \frac{P_{\mathrm{CO}}P_{\mathrm{H_2}}^3}{K_1}\right) \quad (5)$$

$$r_2 = \frac{\mathrm{d}}{\mathrm{d}x}(UC_{\mathrm{CH_4}})_2 = -k_2\left(P_{\mathrm{CH_4}}P_{\mathrm{H_2O}}^2 - \frac{P_{\mathrm{CO_2}}P_{\mathrm{H_2}}^4}{K_2}\right) \quad (6)$$

with the subscripted C symbols representing molar volumes and the subscripted P symbols representing partial pressures. K_1 and K_2 are the equilibrium constants for reactions (1) and (2). The molar volumes and partial pressures are related by the pvT equations typically shown for methane,

$$C_{\mathrm{CH_4}} = \frac{P_{\mathrm{CH_4}}}{zRT} \quad (7)$$

with R the universal gas constant, and the compressibility factor z close to 1.0 in the pressure range of the experiments. U is the superficial gas velocity that is related to the velocity at the reactor entrance U_0 in terms of molar changes due to reaction by,

$$U = \frac{1+s+H+c1+c2+2A}{1+s+H+c1+c2}U_0 = \frac{N_{\mathrm{T}}}{N_0}U_0 \quad (8)$$

where N_0 and N_{T} represent the number of moles as shown. In relation to one mole of methane in the feed, s is the number of moles of steam, H is the number of moles of hydrogen, $c1$ is the number of moles of carbon monoxide, and $c2$ is the number of moles of carbon dioxide in the feed. Along the reactor A is the number of moles of methane reacted and B is the number of moles of carbon dioxide formed in relation to one mole of methane at the reactor entrance. If we now define,

$$\phi_1 = P_{\mathrm{CH_4}}P_{\mathrm{H_2O}} - \frac{P_{\mathrm{CO}}P_{\mathrm{H_2}}^3}{K_1} \quad (9)$$

$$\phi_2 = P_{\mathrm{CH_4}}P_{\mathrm{H_2O}}^2 - \frac{P_{\mathrm{CO_2}}P_{\mathrm{H_2}}^4}{K_2} \quad (10)$$

then the change in partial pressure of methane along the reactor due to both reactions is,

$$\frac{\mathrm{d}}{\mathrm{d}x}(UP_{\mathrm{CH_4}}) = -RT(k_1\phi_1 + k_2\phi_2) \quad (11)$$

and the change for carbon dioxide is given by,

$$\frac{\mathrm{d}}{\mathrm{d}x}(UP_{\mathrm{CO_2}}) = RT(k_2\phi_2) \quad (12)$$

The partial pressure is equal to the product of the mole fraction and the total pressure so that on substitution for the velocity and the partial pressures the two equations become,

$$\frac{\mathrm{d}A}{\mathrm{d}x} = \frac{RTN_0}{PU_0}(k_1\phi_1 + k_2\phi_2) \quad (13)$$

$$\frac{\mathrm{d}B}{\mathrm{d}x} = \frac{RTN_0}{PU_0}(k_2\phi_2) \quad (14)$$

All quantities in the two equations are known from the experimental conditions and measurements except the reaction velocity constants, and by simulating the experimental conditions in the numerical analysis the intention was to estimate the constants. The principal difficulty with the numerical integration is non-linearity so that estimates of k_1 and k_2 are necessary to start the process. The difficulty is reduced by introducing a change in variable $\theta = k_1x/L$, so that

$$\frac{\mathrm{d}A}{\mathrm{d}\vartheta} = \frac{RTN_0L}{PU_0}\left(\phi_1 + \frac{k_2}{k_1}\phi_2\right) \quad (15)$$

$$\frac{\mathrm{d}B}{\mathrm{d}\vartheta} = \frac{RTN_0L}{PU_0}\left(\frac{k_2}{k_1}\phi_2\right) \quad (16)$$

and there is only one unknown parameter, k_2/k_1. A first estimate of k_2/k_1 was adopted and Eqs. (15) and (16) were integrated from the initial conditions $A = 0$, $B = 0$ towards the end reactor values A_F and B_F as measured by the chromatograph until A became $\geqslant A_F$ when the value of B was compared to B_F. If B was sufficiently close to B_F the calculation was stopped, otherwise the Secant method was used to change the value of k_2/k_1 until B was sufficiently close to B_F. At the end of the computation the final value of θ was k_1 to give estimates of both k_2 and k_1.

An example of a computed concentration profile for the experimental reactor is shown in Fig. 7. The concentration profiles were obtained by numerical integration of Eqs. (11) and (12) along the reactor with the reaction constants taken from Eqs. (19) and (20). The initial conditions are those set in the experiment, and the end conditions measured experimentally, are shown and compared with the computed end values. The illustration was chosen so that the differences in the end compositions could be seen at the scale of the graph.

Such calculations were made for all of the sets of experimental measurements. The values of k_1 and k_2 found for each experiment were then examined to establish the influence of temperature, pressure, and composition variables expressed as general rate equations. This was carried out by a functional analysis linked to a non-linear parameter estimation. During the course of the analysis it became apparent that the state of reduction of the catalyst substrate

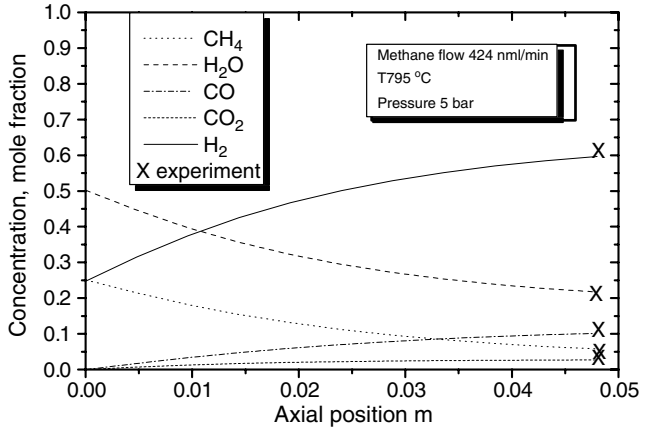

Fig. 7. An example of computed axial concentration distributions.

as characterised by reaction (4) was a significant influence upon the experimental measurements and the scope of the functional analysis was extended to include this factor.

The analysis was carried out by minimising the variance of the measured concentration values about the computed values for all experiments at a pressure of 5 bar. The analysis included changes in temperature, the ratio of steam to methane, the ratio of hydrogen to methane, and the methane flow-rate.

The functional forms associated with the minimum variance are given by Eqs. (17) and (18) that show the explicit effect of temperature and concentration variables at a pressure of 5 bar

$$r_1 = \frac{\mathrm{d}}{\mathrm{d}x}(UC_{\mathrm{CO}}) = k_{10}\exp\left(-\frac{E_1}{RT}\right)\left(P_{\mathrm{CH_4}}P_{\mathrm{H_2O}} - \frac{P_{\mathrm{CO}}P_{\mathrm{H_2}}^3}{K_1}\right)\left(\frac{P_{\mathrm{H_2}}}{P_{\mathrm{H_2O}}}\right) \quad (17)$$

$$r_2 = \frac{\mathrm{d}}{\mathrm{d}x}(UC_{\mathrm{CO_2}}) = k_{20}\exp\left(-\frac{E_2}{RT}\right)\left(P_{\mathrm{CH_4}}P_{\mathrm{H_2O}}^2 - \frac{P_{\mathrm{CO_2}}P_{\mathrm{H_2}}^4}{K_2}\right)\left(\frac{P_{\mathrm{H_2}}}{P_{\mathrm{H_2O}}}\right) \quad (18)$$

Further sets of experimental data were obtained in the same temperature range, but at gauge pressures of 2.5, 7 and 9 bar. The parameter estimation procedures were applied for each pressure. The functional dependences of Eqs. (17) and (18) were found to represent the data accurately at each pressure, but with pressure dependences of both k_{10} and k_{20}. The dependence is shown in Fig. 8 as a graph of the ratio of the reaction velocity constant at an absolute pressure P to the reaction constant at 6 bar absolute pressure. The dependence was found to follow pressure to the inverse power of 2 as indicated on the graph.

On combining this pressure dependence indicated in Fig. 8 with Eqs. (17) and (18) the final forms of the reaction velocity equations are shown as (19) and (20),

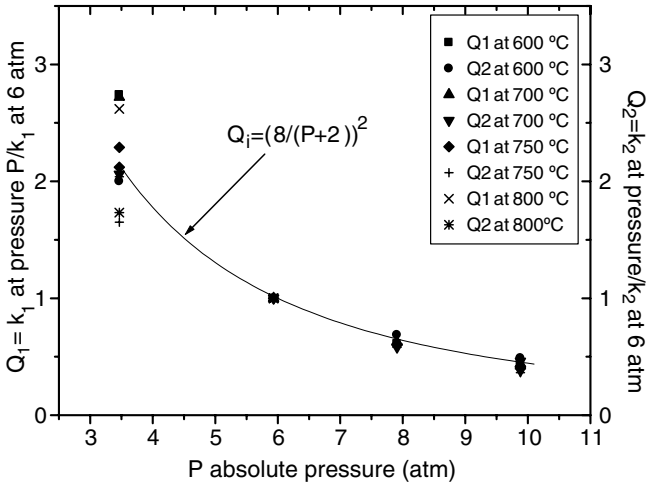

Fig. 8. Pressure dependence of the reaction velocity constants.

$$r_1 = \frac{\mathrm{d}}{\mathrm{d}x}(UC_{\mathrm{CO}}) = k_{10}\exp\left(-\frac{E_1}{RT}\right)\left(P_{\mathrm{CH_4}}P_{\mathrm{H_2O}} - \frac{P_{\mathrm{CO}}P_{\mathrm{H_2}}^3}{K_1}\right) \times \left(\frac{P_{\mathrm{H_2}}}{P_{\mathrm{H_2O}}}\right)\left(\frac{2+P_{\mathrm{ref}}}{2+P}\right)^2 \quad (19)$$

The values of the pre-exponential constant k_{10} and the energy of activation E_1 are, $k_{10} = 6{,}628{,}800$ kmol/s m^3(reactor) atms.^{2} and $E_1 = 17{,}750$ kJ/kmol; P_{ref} is 6 atms. abs.

$$r_2 = \frac{\mathrm{d}}{\mathrm{d}x}(UC_{\mathrm{CO_2}}) = k_{20}\exp\left(-\frac{E_2}{RT}\right)\left(P_{\mathrm{CH_4}}P_{\mathrm{H_2O}}^2 - \frac{P_{\mathrm{CO_2}}P_{\mathrm{H_2}}^4}{K_2}\right) \times \left(\frac{P_{\mathrm{H_2}}}{P_{\mathrm{H_2O}}}\right)\left(\frac{2+P_{\mathrm{ref}}}{2+P}\right)^2 \quad (20)$$

The values of the pre-exponential constant k_{20} and the energy of activation E_2 are, $k_{20} = 5080$ kmol/s m^3(reactor) atms.^{3} and $E_2 = 12{,}250$ kJ/kmol; P_{ref} is 6 atms. The expressions are valid for a range of temperature from 600 to 840 °C, and for a range of pressure from 3.5 to 10 atms. abs.

7. Statistical analysis

An important question is how well do Eqs. (19) and (20) represent the experimental data since the procedures of non-linear parameter estimation and the random nature of the experimental design are not transparent when several variables are involved. To examine this question we use the χ^2 "goodness of fit test" [13], with a comprehensive tabulation of the function provided by Abramowitz and Stegun [14]. The primary data of carbon monoxide and carbon dioxide reactor exit concentrations from 72 experiments are to be compared with concentrations calculated from Eqs. (19) and (20) for the same set of reactor conditions.

In this statistical test the concentration range for carbon monoxide was subdivided and the number of measured concentrations $[\mathrm{CO}]_i$ and the number of corresponding calculated concentrations $[\mathrm{CO}_t]_i$ were found for each subdivision. We wish to examine the hypothesis that the calculated concentrations are drawn from the same population as the measured concentrations. For carbon monoxide the result in tabular form is,

Table of χ^2 for carbon monoxide

Range, mole fraction	0.004–0.022	0.022–0.034	0.034–0.08	0.08–0.10	0.10–0.125
Number of experimental concentrations	10	20	18	16	11
Number of calculated concentrations	4	19	28	13	11

The sum $\chi^2 = \sum(([CO]_i - [CO_t]_i)/[CO_t]_i)^2$ calculated from this table is 0.63. As two parameters were found from the experimental values in the table and the total number of points is fixed, the number of degrees of freedom is $5 - 3 = 2$. From tables of χ^2 [14] the probability that the calculated concentrations are from the same population as the measured concentrations is about 0.75, so affirming the hypothesis and confirming the accuracy of the parameter estimation.

For carbon dioxide,

Table of χ^2 for carbon dioxide

Range, mole fraction	0.006–0.019	0.019–0.024	0.024–0.027	0.027–0.03	0.03–0.036
Number of experimental concentrations	11	18	13	19	11
Number of calculated concentrations	7	25	18	11	11

The sum $\chi^2 = \sum(([CO_2]_i - [CO_{2t}]_i)/[\ CO_{2t}]_i)^2$ calculated from this table is 1.01. As two parameters were found from the experimental values in the table and the total number of points is fixed, the number of degrees of freedom is $5 - 3 = 2$. From tables of χ^2 [14] the probability that the calculated concentrations are from the same population as the measured concentrations is about 0.6, again confirming the hypothesis and the accuracy of the parameter estimation.

8. Conclusions

An experimental investigation of the kinetics of steam reforming of methane over a nickel–alumina catalyst has been carried out in a micro-reactor over a temperature range of 600–850 °C and a pressure range of 2.5–9 atms. gauge. The experiments amounted to 600 h in total. It was found at the end of the experimental programme that measured kinetics were consistent with kinetics measured at the beginning of the programme, and the catalyst was free-flowing at the end of the programme without a trace of sintering or coking.

Experiments using a dynamic method showed that the experimental reaction rates at 700 °C were enhanced for a significant period of time by immediate previous operation at 800 °C. From the experiments and earlier structural and kinetic studies it is deduced that enhanced catalyst reduction experienced at the higher temperature is partly retained for a period at the lower temperature so promoting higher rates of reaction.

The very first experiments showed a high catalytic activity that declined over 60 h of operation to stable values. This period of high catalytic activity appeared to be due to the initial fine dispersion of nickel in manufacture with the subsequent fall caused by a reduction in nickel dispersion under the conditions of solid-state reaction in the catalyst.

Techniques of functional analysis and parameter estimation were applied to the measurements with temperature-enhanced experiments excluded, to obtain rate equations of thermodynamically-consistent form suitable for prediction of full-scale reactors employing the same catalyst. It is shown that the rate equations are statistically consistent with the experimental results.

References

[1] J.R. Rostrup-Nielsen, Catalytic steam reforming, in: J.R. Anderson, M. Boudart (Eds.), Catalysis – Science and Technology, vol. 5, Springer-Verlag, Berlin, 1984 (Chapter 1).
[2] V.M. Twigg, Catalyst Handbook, second ed., Wolf Publishing Co., London, 1989.
[3] W.W. Akers, D.P. Camp, Kinetics of the methane-steam reaction, AIChE J. 1 (1955) 471–475.
[4] I.M. Bodrov, L.O. Apel'baum, M.I. Temkin, Kinetics of the reaction of methane with steam on the surface of nickel, Kinet. Catal. 5 (1965) 696–705.
[5] I.M. Bodrov, L.O. Apel'baum, M.I. Temkin, Kinetics of the reaction of methane with water vapour catalysed by nickel on a porous carrier, Kinet. Catal. 8 (1967) 821–828.
[6] J.R.H. Ross, M.C.F. Steel, Mechanism of the steam reforming of methane over a coprecipitated nickel–alumina catalyst, J. Chem. Soc. Faraday Trans. 1 (1973) 10.
[7] M.E. Agnelli, M.C. DeMicheli, E.N. Ponzi, Catalytic deactivation of methane reforming catalysts, Ind. Eng. Chem. Res. 26 (1987) 1704–1713.
[8] J. Xu, G.F. Froment, Methane steam reforming, methanation and water-gas shift: 1 Intrinsic kinetics, AIChE J. 35 (1989) 88–96.
[9] M.A. Soliman, A.M. Adris, A.S. Al-Ubaid, S.S. El-Nashaie, Intrinsic kinetics of nickel/calcium aluminate catalyst for methane steam reforming, J. Chem. Tech. Biotechnol. 55 (1992) 131–138.
[10] D.J. Gunn, An analysis of convective dispersion and reaction in the fixed-bed reactor, Int. J. Heat Mass Transfer 47 (2004) 2861–2875.
[11] M.A. El-Bousiffi, The dynamics of catalytic steam reforming, Ph.D. Thesis, University of Wales, 1998.
[12] Y. Takemura, Y. Morita, K. Yamamoto, Reduction and oxidation of nickel–aluminium oxide catalysts, Int. Chem. Eng. 6 (1966) 725–729.
[13] C.E. Weatherburn, Mathematical Statistics, Cambridge University Press, 1968.
[14] M. Abramowitz, I.A. Stegun, Handbook of Mathematical Functions, Dover Press, 1965.